ELSEVIER

Journal of Chromatography A, 667 (1994) 257–270

JOURNAL OF CHROMATOGRAPHY A

Computer simulation for capillary zone electrophoresis A quantitative approach

Sergey V. Ermakov[☆], Pier Giorgio Righetti*

Faculty of Pharmacy and Department of Biological Sciences and Technologies, University of Milan, Via Celoria 2, Milan 20133, Italy

(Received November 15th, 1993)

Abstract

The simulation results for peak quantification and for describing a peak shape and transit time in capillary zone electrophoresis (CZE) are described. For peak quantification, two approaches are described and compared: a differential and an integral method. An attempt is made at describing by computer simulation the *temporal dependence* of a detector signal, as typical of output data in experimental runs, instead of as a *space distribution*, as offered by earlier computer modelling. The peak shape and transit times are evaluated as a function of the concentration of sample within a single peak and the presence of several analytes in the injected sample mixture. The phenomena of peak fronting and tailing due to conductivity differences and anomalies of migration time due to the effect of absolute sample molarities on the degree of ionization in mixtures of weak and strong electrolytes can be correctly assessed and predicted by the present computer program. Unlike previous computer modelling performed by different workers, good *quantitative* coincidence of simulated and experimental results for real operating parameters used in everyday practice was demonstrated. This is the first time that an approach to "dry chemistry", prior to actual "wet" runs, has been performed under real experimental conditions in CZE, as is typically done in high-performance liquid chromatography.

1. Introduction

The evolution of chemical species in free fluid solution under the effect of an electric field, known as electrophoresis, has been the subject of computer modelling for more than 10 years [1]. During these years a unified mathematical model for electrophoresis was developed; with it four basic migration modes: zone electrophoresis, isotachophoresis, isoelectric focusing and moving boundary electrophoresis were simulated. The modelling started from the relatively simple problem of studying the evolution of a boundary between two weak monovalent electrolytes [2,3]; later it was extended to multicomponent systems and proteins [4–7]. These results were summarized by Mosher *et al.* [8]; an extensive review of work on computer simulation in electrophoresis has also been published [9].

However, in the field of electrophoresis, there is still some mistrust of computer modelling. Probably this can be explained first by the absence of a correct quantitative comparison between experimental and simulated data, as all of the work mentioned above gave only quali-

* Corresponding author.

☆ Permanent address: Keldysh Institute of Applied Mathematics, Russian Academy of Sciences, Miusskaya Sq. 4, 125047, Russian Federation.

0021-9673/94/$07.00
SSDI 0021-9673(94)00035-8

tative information. Direct quantitative comparison assumes that simulations should be performed for parameters corresponding to the real experimental conditions and also both experimental and calculated electropherograms should be presented on the same plot with the same coordinate system. There is no doubt that previous simulations helped to reveal and explain a lot of details in separation patterns, while providing the necessary background for future research. However, in recent years, electrophoretic methods have been developed to such an extent that the reproducibility of experimental results with only 2–3% errors became the normal practice. In this situation a pure qualitative description could not be considered satisfactory. At the same time, new achievements in experimental science created the basis for an accurate verification of the mathematical model [8] used in simulations. This circumstance became the main stimulating motive for starting work on quantitative comparisons of experiment and computer simulation. Among other factors that impinged on this work were the progress in high-performance capillary electrophoresis (HPCE), offering excellent reproducibility with short analysis times and computer data processing, and the development of efficient, high-resolution numerical algorithms [10], allowing for simulation of real experimental conditions.

There were several problems that made impossible the direct comparison of experimental and computer modelling results earlier. One of them is the simulation of experiments with input parameters that do not correspond to the actual conditions used in practice. We mean here not the inevitable restrictions implied by the mathematical model such as isothermal conditions, one-dimensional consideration, constant pK and mobility values. Simply in most of the work the simulations were performed for input parameters that were known in advance to be far from real [6]. Some of the reasons for this discrepancy were that computer simulations did not have as a goal the comparison of experimental and simulated results, and that available numerical algorithms did not allow solutions to be obtained at reasonable computational expense. Attempts to use the simplified models allowing for the analytical solutions usually gave predictions that might be considered only as a first approximation to reality [11,12].

The other cause of difficulties in comparison is connected with different ways of data presentation in experiment and in computer simulations. In the experimental runs the output data are given in the form of a *temporal dependence* for the detector signal whereas computer simulation results are usually presented as a *space distribution* along the electrophoretic column axis. The comparison of spatial distribution and temporal signal is not so obvious as it may seem at first. For example, in temporal electropherograms, the peak width for sample species depends on the migration velocity of each component [13]. Another aspect complicating the data comparison is that in experiments a UV absorbance signal is obtained, whereas simulations are performed in terms of concentrations. Two standard procedures are mostly used for quantifying the electropherograms: according to the peak height and according to the peak area [14]. Although there are no substantial difficulties in recalculating the absorbance electropherograms into concentration profiles and then plotting them on the same axis system, usually this is not done.

It is worth mentioning that the sampling techniques are also of importance for quantitative analysis. Electropherogram quantification by means of peak areas needs accurate information on analyte mass; in addition, for simulation purposes, one should know precisely the amount of sample injected. The problem of quantitative injection and the advantages and drawbacks of electrokinetic and hydrodynamic modes have been considered previously [14,15].

In this work dealing with the comparison of experimental and simulated results we tried to overcome the above problems. The main aim of this study was to perform computer simulation of electrophoretic runs for parameters as close as possible to those of the real experiment. The shape of the concentration profiles for sample species and their migration time characteristics were considered as the subject for comparison. Weak monovalent acids and bases with good UV absorbance were the sample constituents. We took these substances as their mathematical

description is the simplest compared with others. They are completely characterized by only two constants, the pK value and the ionic mobility, which are usually well known. For experimental runs we used an HPCE unit run in the capillary zone electrophoresis (CZE) mode. HPCE provides a unique opportunity for comparison, because it gives highly reproducible results ready for computer handling within a few minutes. Another unique feature of this technique is the use of thin capillaries, for which it is relatively easy to maintain isothermal conditions in a buffer. The thermal problem in this instance is reduced to temperature corrections for substance ionic mobilities. The influence of hydrodynamics on separation patterns is caused by the effect of electroosmotic flow. Since it has a uniform "flat" velocity profile, it does not cause an additional zone distortion. It can be accounted for by adding the electroosmotic velocity to the electrophoretic migration. All these circumstances significantly simplified the mathematical description compared with column or free flow electrophoresis.

We displayed the results, both experimental and computed, as a detector signal, *i.e.*, temporal dependence of concentration, scaled to the same axis system. For this purpose the two quantification methods mentioned above were tested. The use of buffer systems with different pH values allowed the study of the evolution of samples with full and partial dissociation comprising one or more chemical species. Experimental and computer simulation results were compared with analytical solutions [11].

2. Theory

For computer simulations we used a mathematical model based on mass and charge conservation laws, the assumption of local electroneutrality and chemical equilibria equations described previously in detail [16]. The only modification of this model was the explicit introduction of electroosmotic velocity to the convective terms in mass transport equations, describing the evolution of electrolyte constituents. A high-resolution finite-difference scheme [10] for solving the non-linear partial differential equations underlaid the numerical algorithm used in simulations. It exhibited excellent results when it was compared with the other algorithms used in electrophoresis simulations [17].

The model mentioned above assumes isothermal conditions during the experiment, so it is necessary to take the following run parameters, for which this approximation holds true. Thermal problems connected with capillary electrophoresis have been extensively examined in recent years [18–21]. The temperature distribution in solution is determined by the amount of Joule heat, G, generated per unit capillary length [18]. As has been shown [19], under normal operational conditions the radial temperature profile could be considered to be parabolic with good accuracy, so the radial temperature difference, δT, between the capillary axis and its wall can be estimated as [18]

$$\delta T = \frac{GR_1^2}{4k_1} \tag{1}$$

where R_1 is the internal capillary radius and k_1 is the thermal conductivity of buffer solution (water). As Joule heat generation is given by

$$G = \frac{VI}{\pi R_1^2 L} = \frac{EI}{\pi R_1^2} \tag{2}$$

Eq. 1 can be rewritten in the form

$$\delta T = \frac{EI}{4\pi k_1} \tag{3}$$

where V is applied voltage, I is current, L is the total length of the capillary and E is the field strength. For estimates let us suppose that the field strength and current do not exceed $3 \cdot 10^4$ V/m and 15 μA, respectively, and the thermal conductivity of the buffer solution is equal to that of water, $k_1 = 0.609$ (at $T = 27$°C) [20]. Then the radial difference $\delta T \approx 0.06$, so we can neglect it and consider the temperature over the capillary cross-section to be uniform.

It is difficult to measure the temperature directly in solution within a capillary so only the temperature of the medium surrounding the

capillary is usually known. The problem of how to determine precisely the temperature within the capillary for the HPCE units has been described [21]. For calculating the excess of temperature in the buffer, ΔT, compared with the temperature of the coolant (air) we use the simple equation [21]

$$\Delta T = \frac{VI}{2\pi Bi_{OA} k_1 L} = \frac{EI}{2\pi Bi_{OA} k_1} \quad (4)$$

where Bi_{OA} is the overall Biot number, which specifies the outer heat transfer from the capillary. For the Waters Quanta 4000 HPCE unit, which we used in our experiments, this parameter was determined as $Bi_{OA} \approx 0.055$ [21]. Taking this Biot number and the same parameters as chosen previously, one can easily calculate $\Delta T \approx 2.1$. For such small deviations it is possible to consider ionic mobility to be linearly dependent on temperature and to use simple corrections assuming an increase of 2% for every 1°C increase.

In order to compare the simulated results and the experimental electropherograms in terms of concentration, one should establish somehow a correspondence between absorbance as a function of time $f(t)$ and concentration $c(t)$. One of the ways is to construct a calibration function relating absorbance and sample concentration. For this purpose let us consider a function $k(c)$ which equals the sample concentration c divided by absorbance f, *i.e.*, $k(c) = c/f$. Measuring $k(c)$ for several c values over the range of concentrations expected in experiments, we then approximate these data by one of the best fit curves $\bar{k}(c)$ (linear, polynomial, exponential, etc.). When $\bar{k}(c)$ has been calculated, the following equation is obtained:

$$\bar{k}(c) = c(t)/f(t) \quad (5)$$

with c as an unknown and t as an argument. When $\bar{k}(c)$ is a linear function of concentration, $\bar{k}(c) = \alpha c + \beta$ (α, β = constants are the best fit parameters), the equation has a solution

$$c(t) = \frac{\beta f(t)}{1 - \alpha f(t)} \quad (6)$$

Determining α and β from best fitting and using Eq. (6), one can easily transform the absorbance curve into a concentration profile. For $\alpha = 0$ the simplest relationship between c and f is derived as $c(t) = \beta f(t)$, which resembles the Lambert–Beer law. For more complex functions $\bar{k}(c)$, Eq. 5 can be solved numerically.

The crucial point in such a technique is a calibration procedure from f to c. It can be performed by injecting a sample plug of known concentration and observing its UV response. At the moment of detection, in addition to absorbance, which is monitored by a detector, an experimenter needs to know the precise value of the sample concentration at this point. Usually the concentration profile for a short sample pulse has a rectangular form (or close to it) with a plateau of known concentration only for a limited period of time just after injection. Travelling along the capillary and being distorted by a number of dispersive mechanisms [22], by the moment of detection the sample zone has a symmetrical gaussian or skewed shape. The concentration at the peak apex is unknown and there is a probability that it can be different from the initial value. In order to avoid the uncertainty in concentration at the detection point we offer the following procedure. It is necessary to inject the sample continuously until it reaches the detector. The absorbance profile $f(t)$ would then have the shape of a step (Fig. 1), with the lower level f_l corresponding to zero concentration and the upper level f_u corresponding to the concentration of the sample. There is a relatively small transition region due to the action of diffusion where the absorbance changes from f_l to f_u. The difference $f_u - f_l$ gives the relative absorbance value corresponding to the sample concentration. It is clear that the sample should be injected hydrodynamically, as during the electrokinetic injection the electromigration dispersion due to the variances in conductivity may significantly spread the transition region.

Another way to quantify the UV absorbance electropherogram in terms of concentration is to take the total mass of the sample m as a reference point. At the detection point it is calculated as

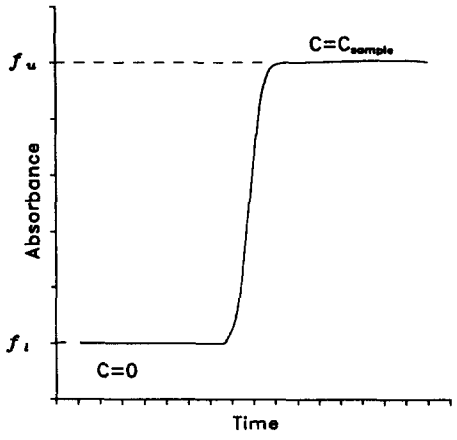

Fig. 1. Absorbance profile with continuous sample loading for calibration procedure. Absorbance level f_l corresponds to pure buffer and f_u corresponds to absorbance by a substance with concentration $c = c_{sample}$.

$$m = \pi R_1^2 \int_0^{+\infty} v(t)c(t)\,dt = \pi R_1^2 \bar{v} \int_0^{+\infty} c(t)\,dt$$

$$= C_0 \int_0^{+\infty} c(t)\,dt \quad (7)$$

or

$$m/C_0 = \int_0^{+\infty} c(t)\,dt \quad (8)$$

where $v(t)$ is an instantaneous velocity of sample zone at the detection point at moment t and $\bar{v}$ is its average velocity. The zeroth moment of the electropherogram also gives the value corresponding to the mass of the sample:

$$F_0 = \int_0^{+\infty} f(t)\,dt \quad (9)$$

Comparing Eqs. 8 and 9 and assuming the linear dependence $c(t) = kf(t)$ with k = constant, one can easily derive that

$$\int_0^{+\infty} c(t)\,dt = \frac{m}{F_0 C_0} \int_0^{+\infty} f(t)\,dt$$

or

$$c(t) = \frac{m}{F_0 C_0} f(t) \quad (10)$$

The value of m/C_0 is calculated from the simulated profile $c(t)$ and F_0 from the experimental electropherogram.

As in the first method the absorbance profile is recalculated into a concentration profile using a number of calibration points and in the second method the only integral characteristic (area under the curve) is used, from here, for the sake of brevity, we shall refer to the first method of quantification as a differential and to the second method as an integral method.

3. Experimental

All chemicals used were of analytical-reagent or research grade. Most of them were purchased from Merck (Darmstadt, Germany), picric acid from Carlo Erba (Milan, Italy) and acrylamide from Bio-Rad Labs. (Richmond, CA, USA). Fused-silica capillaries of length 37.7 cm with nominal I.D. 75 μm were obtained from Polymicro Technologies (Phoenix, AZ, USA). The detection path for this capillary was 30.0 cm. We performed experiments on a Waters Quanta 4000 capillary electrophoresis system (Millipore, Milford, MA, USA) equipped with a personal computer running under Baseline 810 software (Dynamic Solutions, Division of Millipore). The unit was equipped with a UV absorbance detector (mercury lamp, 254-nm filter) and it worked in a voltage-stabilized regime of 10 kV. The air temperature within the capillary unit and the magnitude of the electric current were also monitored during the experiments. Typical values for temperature lay within the range 26–28°C. For injection, a sample hydrostatic loading method was used, as the amount of a sample loaded did not depend on the velocity of electroosmotic flow and the electrophoretic mobility of the sample. During injection, lasting 10 s, the sample volume loaded was *ca.* 20.6 nl, which corresponded to a sample plug length of 0.466 cm within the capillary. The total amount of sample depended on the particular concentra-

tion. Between successive runs the capillary was rinsed only with buffer for 5 min. In each series of experiments we performed one control run in order to measure the velocity of electroosmotic flow. For this purpose a small pulse of 5 m*M* acrylamide as a neutral marker was injected. According to its migration time the velocity of electroosmosis was calculated.

Computer simulations were performed on an AT 486 personal computer running at 33 MHz. The computer code was written in Fortran algorithmic language using the Microsoft Fortran (Version 5.1) Development System, as used earlier for simulation of capillary electrophoresis [16]. For this work we changed the method of data presentation, giving the concentration profiles as a temporal signal at a given point of the capillary. During simulations a finite-difference grid covered only that part of capillary where sample species were located at a given time moment. This helped to reduce the computational expenses. Initial conditions specified the distribution of all sample and buffer components, their ionic mobilities, p*K* values, capillary geometry, applied voltage and temperature. For handling the experimental electropherograms a special computer program was written, which allowed us to cut the desired part of the electropherogram, to calculate the baseline level, subtract it, if necessary, calculate the moments and finally recalculate the electropherogram in terms of concentration.

4. Results

The weak monovalent picric and salicylic acids were chosen as sample species. We took negatively charged substances in order to minimize the probability of sample adsorption on the capillary wall, because as a rule it is negatively charged owing to ionization of silanol groups. Buffer solutions were 20 m*M* formic acid titrated with NaOH to pH 3.0 or 20 m*M* acetic acid titrated with NaOH to pH 5.0. The concentration of the sample species was within the range 0.02–10 m*M*. The input data for the substances used in the simulation are summarized in Table 1. It is worth noting that there are some discrepancies in data given by different sources. For example, the ionic mobility of salicylic acid at 25°C according to ref. 23 is $3.73 \cdot 10^{-8}$ m^2 V^{-1} s^{-1}, but in ref. 24 the value $3.53 \cdot 10^{-8}$ m^2 V^{-1} s^{-1} is given. The difference is more than 5%, which cannot be considered as negligible, especially for quantitative analysis.

Table 1
Input data for computer simulations

Substance	pK_a	μ (10^{-8} m^2 V^{-1} s^{-1})
Acetic acid	4.75	4.24
Formic acid	3.75	5.66
Salicylic acid	2.937[a]	3.73
Picric acid	0.38	3.15
Na^+	–	5.19
H^+	–	36.2
OH^-	–	20.5

All values at 25°C from ref. 23 except where indicated otherwise.
[a] Data from ref. 24.

The first series of experiments was performed with picric acid as a sample in acetate buffer. We started with the calibration procedure described under Theory, which was necessary for differential quantification method. Samples with concentrations of 0.02, 0.1, 0.5, 1, 5 and 10 m*M* were used. The results of the calibration are presented in Fig. 2 where the measured points and best fit line $\bar{k}(c)$ are plotted. The best fit line was approximated by a linear dependence $\bar{k}(c) = 2.11c + 22.53$. This calibration graph was used in the quantification of experimental electropherograms.

The experimental electropherograms (solid lines) together with computer simulation results (dashed line) are plotted for six different sample concentrations, $c_0 = 0.02$, 0.1, 0.5, 1, 5 and 10 m*M*, in Fig. 3A, B, C, D, E and F, respectively. The two different experimental electropherograms in each panel represent different quantification methods: The solid lines without symbols are the results obtained by the differential method and those with solid circles are the data for the integral quantification method. The experimental and calculated electropherograms

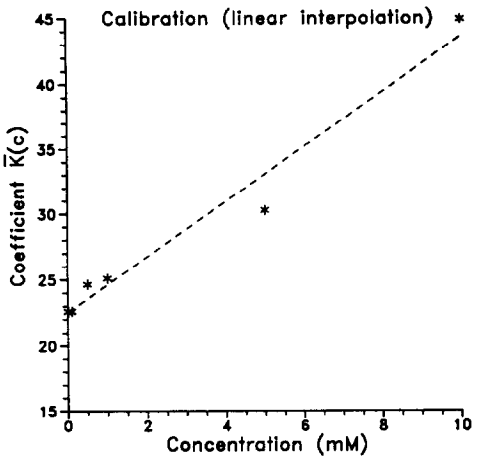

Fig. 2. Calibration graph for picric acid: dependence of parameter $k(c) = f/c$ on sample concentration. * = Experimental points; dashed line = best fit line.

demonstrate good qualitative and quantitative agreement when the shapes of the concentration profiles, migration times or maximum concentration values are compared. The simulated profiles have small false spikes near the sharp concentration boundaries. They should not be taken into account because of their purely computational origin.

It can be clearly seen that for sample concentrations $c_0 = 0.02$ and 0.1 m*M* (Fig. 3A and 3B), which are low compared with that of the background electrolyte (20 m*M*), the sample zone is subjected mainly to diffusion dispersion. Its concentration profile is close to gaussian. The slight skew in the experimental profiles can probably be explained by the interaction with the wall. Starting from $c_0 = 0.5$ m*M* (Fig. 3C), electromigration dispersion due to conductivity differences between the sample zone and background electrolyte plays the major role. It changes the zone shape to a typical triangular form. This transition in sample evolution from a diffusion-controlled regime to a state with a predominant influence of electromigration dispersion was confirmed by computer simulations. Another phenomenon observed in the experiments and proved by simulations is the decrease in migration time with increase in sample concentration. The migration time measured according to the front boundary position decreased from *ca.* 6.1 min ($c_0 = 0.02$ m*M*, Fig. 3A) to 5.4 min ($c_0 = 10$ m*M*, Fig. 3F) in experiments compared with 5.8 and 5.2 min, respectively, in simulations. The differences are 0.7 min and 0.6 min, respectively. This phenomenon is explained by the fact that the velocity of sample particles is higher in the regions with higher concentration [25]. In this case the sample "triangle" has sharp leading edge and tailing rear boundary, as observed in the figures.

Careful analysis of the data reveals some differences between simulation and experiment. Among them there are features observed in all figures. First, it should be noted that the differential quantification method gives a better coincidence with simulated results for the sample peak height, but it exaggerates the total area under the curve. The difference in peak concentration was of the order of 8%, whereas the difference in peak area reached 30%. Second, the sample zones in experiments are always wider than those predicted in simulations. Third, the migration time given by simulations is less than experimentally observed. Its value was calculated as a migration time for the sample centre of mass using moment analysis [26].

For migration times the deviation of experimental and simulation data did not exceed 5% and the discrepancy can be explained by a number of factors. As we have already noted, the input data for ionic mobilities and p*K* values taken from the literature are known to have some errors. Usually their determination within a deviation of ±3% may be considered to be reasonable. The next factor affecting the sample migration time is electroosmosis. The velocity of electroosmotic flow was about 20% of that of the sample. However, this value might vary from run to run and, probably, the actual velocity in each experiment was slightly different from that used in simulations. A further cause of the discrepancy is the error in temperature data measured within the HPCE unit. It may also make some contribution to the total error.

It is more difficult to find reasonable explanations for the first two discrepancy features. The excessive width of the sample zone and its

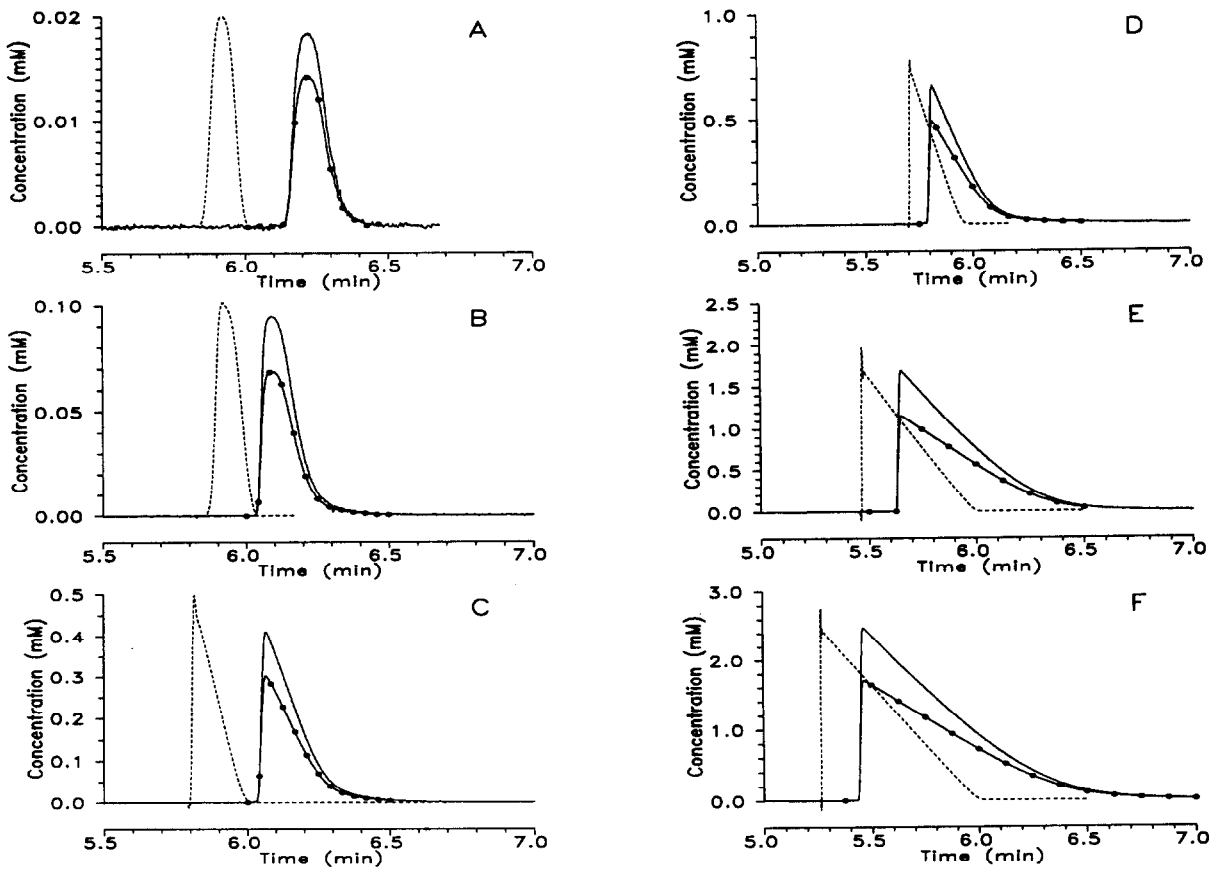

Fig. 3. Comparison of computer simulation and experimental electropherograms. Buffer, 20 m*M* acetic acid–NaOH (pH 5.0); sample, picric acid of concentration (A) 0.02, (B) 0.1, (C) 0.5, (D) 1.0, (E) 5.0 and (F) 10.0 m*M*. Here and also in Figs. 3–6 the solid line with symbols represents experimental data obtained by the differential method and the solid line without symbols represents experimental data obtained by integral method. The dashed line is the computer simulation.

excessive mass might mean that the actual injected mass was larger than that used as input data in calculations. However, this suggestion was not confirmed in the subsequent series of experiments with this and the other substances. There is an alternative reason explaining the additional sample zone dispersion observed in all experiments. We assume that despite the negative charge of sample species there was still some adsorption on the capillary walls. This might lead to additional sample spreading and to its lower effective mobility, as part of the time it rested on the wall surface. This provides one more possible cause for the increased migration time. Adsorption on the wall was possible because the wall surface charge was small, as shown by a weak electroosmotic flow, the velocity of which is directly proportional to the surface charge.

The next series of experiments and computer simulations was performed with picric acid as a sample, but using 20 m*M* formate buffer (pH 3). The experimental and calculated sample concentration profiles are plotted in Fig. 4A, B and C for initial sample concentrations of 1, 5 and 10 m*M*, respectively. The concentration profiles have a typical triangular shape, but unlike the previous instance the front boundary is dispersive whereas the rear boundary is sharp. This shape helps to reveal the additional dispersion mechanism, affecting the sample zone. It appeared in some experimental electropherograms as a tail adjacent to the rear boundary of the

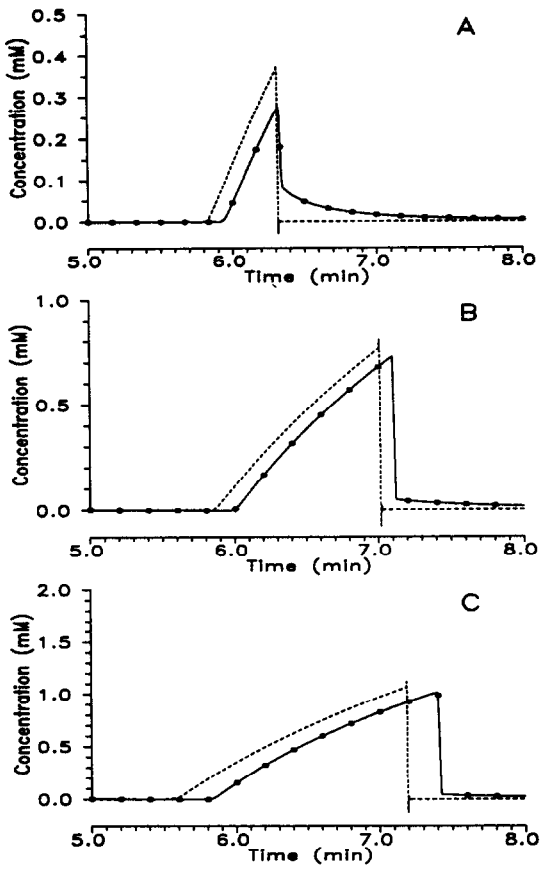

Fig. 4. Comparison of computer simulation and experimental electropherograms. Buffer, 20 m*M* formic acid–NaOH (pH 3.0); sample, picric acid of concentration (A) 1.0, (B) 5.0 and (C) 10.0 m*M*. For explanation see also Fig. 3.

sample zone. The concentration profile has an unusual bend at the point where the almost vertical part of the profile is followed by a smooth curve with concentration decreasing to zero. The last part of the profile is absent in simulated profiles, as the mathematical model does not account for this phenomenon. We assume that this additional dispersion is caused by sample adsorption. On the previous electropherograms this tailing phenomenon was obscured by tailing due to electromigration dispersion. We suspect it only from the excessive width of the sample zone. The relative effect of adsorption on the total sample transport depends on its concentration. For small concentrations (Fig. 4A) this tail contains a considerable part of the sample mass, which results in a decrease in the concentration maximum at the profile apex. For higher concentrations (Fig. 4B and C) the relative influence of adsorption is less and the shape of the experimental electropherograms approaches the simulated plot. In this series, the experimental electropherograms obtained with the use of differential and integral quantification methods virtually coincide. As in the preceding runs, the migration time observed in experiments is slightly longer than that predicted by computer simulations.

The above experiments involved a sample substance that was almost fully ionized, because for picric acid $pK = 0.38$ while the buffers used had pH 5 and 3. It was interesting to investigate the evolution of a sample with a pK value close to the pH of the buffer electrolyte, when the degree of its dissociation may change significantly within the sample zone. Salicylic acid dissolved in 20 m*M* formic acid buffer (pH 3.0) was a good candidate for this purpose. The results of experiments and computer simulations for sample concentrations of 1, 5 and 10 m*M* are plotted in Fig. 5A, B and C, respectively. The shapes of experimental and calculated concentration profiles are quite similar especially for larger concentrations. The effect of adsorption is noticeable only for the 1 m*M* sample, which gave a small tail behind the rear zone boundary (Fig. 5A). The difference in the absolute values of the migration time between experiment and simulations is greater than for the previous series. However, this error divided by the total migration time is approximately the same, as the effective mobility for salicylic acid was lower.

In order to evaluate the quality of predictions made by means of computer modelling they were compared with theoretical results obtained using the analytical solution [11]. Fig. 6A and B present the concentration profiles of picric acid as obtained by experiment, computer simulation and analytical solution. Fig. 6A shows the electropherograms for the sample in formate buffer and Fig. 6B for that in acetate buffer. The initial sample concentration was 10 m*M*. Experimental and simulated data were taken from Figs. 4C and 3F, respectively, the concentration profile de-

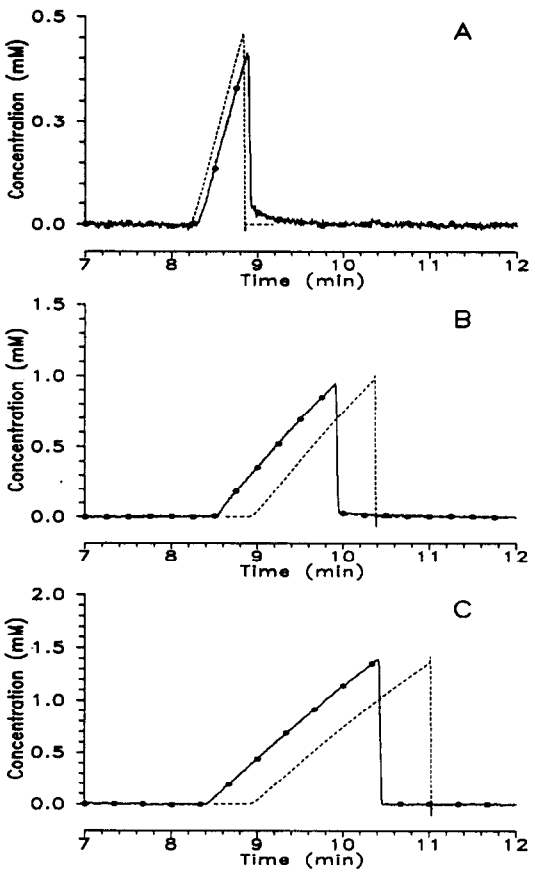

Fig. 5. Comparison of computer simulation and experimental electropherograms. Buffer, 20 m*M* formic acid–NaOH (pH 3.0); sample, salicylic acid of concentration (A) 1.0, (B) 5.0 and (C) 10.0 m*M*. For explanation see also Fig. 3.

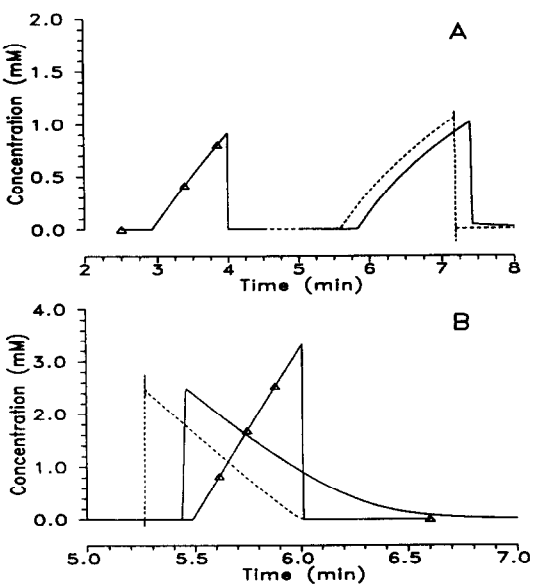

Fig. 6. Comparison of experimental and computer simulation and results with analytical solution [11]. (A) Corresponds to experimental results presented in Fig. 4C; (B) corresponds to experimental results presented in Fig. 3F. △ = Electropherogram calculated using ref. 11. For explanation see also Fig. 3.

rived from ref. 11 are marked with triangles. For the sake of clarity only one experimental electropherogram representing the differential quantification method is presented. As can be seen, the analytical results from ref. 11 are far from the experimental and computer-simulated data with formate buffer (Fig. 6A) the shape of electropherogram predicted by analytical solution is similar to that observed experimentally, but the sample migration time is halved. Such a large difference is explained by simplifications assumed in the mathematical model for which the analytical solution was obtained. It neglects the contribution of H^+ ions to the specific conductivity despite the fact that for this particular buffer solution it reaches 46%. Owing to the increase in sample velocity its zone passes through the detector in a shorter time, so the zone width is less than that given by computer simulation (Fig. 6A).

With acetate buffer the sample migration time predicted by analytical solution [11] agrees well with the experimentally observed data (Fig. 6B). For 20 m*M* buffer (pH 5) the contribution of hydrogen and hydroxyl ions to the specific conductivity is negligible, so they may be excluded from consideration. At the same time, the shape of the concentration profile given by analytical solution [11] is wrong. The "direction" of sample zone asymmetry is opposite to that of the experimental and calculated electropherograms. In ref. 11 the "direction" of peak asymmetry depends on the sign of the difference between the sample effective mobility $\bar{u}_S$ and that of background electrolyte co-ion $\bar{u}_A$. When $\bar{u}_S > \bar{u}_A$ the

zone front boundary is dispersive whereas the rear boundary is sharp (as in Fig. 6A), and for $\bar{u}_S < \bar{u}_A$ the situation is the opposite. For this particular case when pH = 5, $\bar{u}_S = 3.15 \cdot 10^{-8}$ m^2 V^{-1} s^{-1} and $\bar{u}_A = 2.71 \cdot 10^{-8}$ m^2 V^{-1} s^{-1}, *i.e.*, $\bar{u}_S > \bar{u}_A$, which corresponds to the shape of the concentration profile. However, more correct predictions are based on the consideration of specific conductivity variations. If it is higher in the sample zone compared with that of the background electrolyte, the concentration profile would have a "direction" of asymmetry analogous to that in Fig. 6A. It would have the opposite "direction" in another case. The latter is realized in the experiment shown in Fig. 6B. Thus, in this particular run the analytical results obtained in ref. 11 have features different from the experimental data on both quantitative (compare the maximum sample concentrations at the peak apex) and qualitative levels (the shape of the concentration profile).

We also performed experiments with samples consisting of two different substances. It was interesting to study how the computer simulation can predict the evolution not only of a solitary zone but also the interaction of sample components when there are several of them. This interaction is significant if the concentration of the sample species is comparable to that of the buffer.

Experimental and calculated electropherograms for 2.5 m*M* picric acid + 5 m*M* salicylic acid sample in 20 m*M* formate buffer (pH 3.0) are plotted in Fig. 7. Parts of the curves representing salicylic acid are marked with circles. For both substances the simulated and experimental data agreed fairly well. Note that the migration time for salicylic acid is slightly longer than that observed in Fig. 5B for the same concentration when the sample consisted solely of this substance. Its front boundary reached the detector at $t_b \approx 9.3$ min, whereas for the pure substance $t_b \approx 8.5$ min. Simultaneously for picric acid the migration time hardly changed. At the beginning of the separation the presence of stronger picric acid in the sample decreases the dissociation of salicylic acid. Hence when the sample substances are still not spatially separated, the salicylic acid has a lower effective mobility than for the pure substance. This effect is confirmed by computer simulation results.

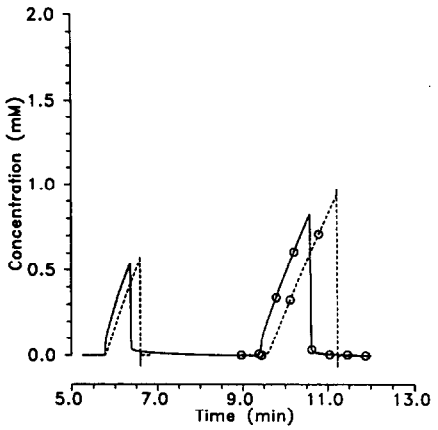

Fig. 7. Comparison of computer simulation and experimental electropherograms. Buffer, 20 m*M* formic acid–NaOH (pH 3.0); sample, 5 m*M* salicylic acid–2.5 m*M* picric acid. Solid lines represent experimental data and dashed lines simulated data. Lines without symbols are for picric acid; O = salicylic acid.

5. Discussion

From the present computer modelling and experimental results, it is clear that there are several factors influencing both the peak shape and its transit time in CZE. Among them are the reproducibility of electroosmotic flow (due to the degree of ionization of silanols on the inner surface), the potential interaction of analytes with the silica wall, the conductivity difference between the analyte and the surrounding background electrolyte and the presence of several analytes in the injected sample mixture. It has been impossible here to account for all of these aspects, which will need more extensive studies and more complex algorithms even for an approach to a solution. For example, there is still a hot debate on the reproducibility of the electroosmotic flow. As reported by Lambert and Middleton [27], among other factors, it seems that μ_{eos} also depends strongly on the precondi-

tioning of the fused-silica column. The μ_{eos} values obtained from a column previously exposed to acidic conditions are consistently lower than those using columns previously exposed to alkaline conditions. This hysteresis phenomenon is consistent with a slow equilibration of the surface, and it might take as long as a few weeks for the process to reach a plateau. This study suggests that there are still some phenomena responsible for μ_{eos} that are not yet fully understood.

We also have not investigated here the potential interaction of analytes with the capillary wall (be it by ionic or silanophilic or even hydrophobic interactions); this is a complex problem requiring the simultaneous solution of electrophoretic mass transport equations combined with equations describing different types of chromatographic interaction with the wall. What we have addressed here is how the peak shape and transit times are affected by the last two factors: (a) the concentration of a sample within a single peak and, as a consequence, the conductivity difference between the analyte and surrounding background electrolyte; and (b) the presence of several analytes in the injected sample mixture. Phenomenon (a) was recognized long ago by Everaert's group in their pioneering work on CZE [25]. Qualitatively, this mechanism of band broadening can be described as follows: if the conductivity in the sample zone (A) is lower than that in the background electrolyte (B), there will be a higher voltage gradient in A, resulting in dispersion of the rear boundary and sharpening of the front boundary; this phenomenon is called "tailing" (*e.g.*, see Fig. 3 D–F). Conversely, if the conductivity in A is greater than in B, the voltage gradient in A will be lower than in B, and molecules of analytes retarded in the front part of the sample zone will be accumulated on the rear boundary. This will result in sharpening of the rear boundary and dispersion of the front boundary (a phenomenon called "fronting", *e.g.*, Figs. 4 and 5A–C). Hjertén [22] derived a simple approximate expression describing this conductivity-induced band broadening quantitatively. Note in addition that our model correctly predicts the shape of the peaks and can describe with a very good approximation both fronting and tailing; conversely, the model proposed by Šustáček *et al.* [11] fails in some instances (see Fig. 6B).

Phenomenon (b) (how different analytes in a single zone influence each other's migration) is more subtle and deserves further comments. A case in point is represented by the mixture of picric acid (a stronger acid, $pK = 0.38$) and salicylic acid (a weaker acid, $pK = 2.94$). When present in the same zone, the stronger acid suppresses the ionization of the weaker acid, which results in a retardation of salicylic acid migration (see Fig. 7). This phenomenon, often overlooked, might be an important cause of irreproducibility of peak transit times, often blamed on fluctuations of electroosmotic flow. As a final remark, an important cause of peak irreproducibility is the molarity of the sample injected. As seen in the series of experiments in Fig. 3A–F, at progressively higher molarities of injected sample (0.02–10 m*M* picric acid), the migration time, as measured from the position of the front boundary, decreases substantially from 6.1 to 5.4 min, a phenomenon first described by Mikkers *et al.* [25]. Here too our computer model can predict and simulate fairly accurately such non-ideal behaviour.

We can summarize all the above observations by noting that, in CZE, nothing can be considered constant any more, as numerous phenomena affecting peak shape and transit time are strongly dependent on the molarity of sample present in a zone (and distortions are clearly visible already, for small analytes, at a level of 0.1 m*M*; see Fig. 3B). This is not surprising, and goes back to theories proposed at the turning of the century by Van't Hoff and Arrhenius and later developed by Debye and Hückel. The concentration of an analyte in solution affects both strong and weak electrolytes. In the former instance it changes the activity coefficient (γ); in the latter it alters the degree of dissociation (α, and ultimately the p*K* value of the substance). There are two ways to solve these problems: the first, as presented here, by proposing novel algorithms that can predict and model such phenomena, so that peak transit times and

shapes can be accurately described at any (reasonable) value of injected analyte. The second way is to exploit modern techniques labelling an analyte with a fluorescent tag (having a very high quantum yield) and induce such fluorescence by a laser beam: zeptomole sensitivity has been claimed; in fact, even as low as 500 yoctomol [28], which essentially would allow an almost infinite dilution of molecules in the sample peak. At such incredible dilutions, it is essentially guaranteed that the peak will have an ideal behaviour. Modern computer simulators should implement all such deviations from ideal behaviour, in order to serve as a user-friendly tool in laboratory practice. For example, also using immobilized pH gradients, where weak acids and bases are grafted on to a polyacrylamide matrix to create any pH gradient in the pH range 2.5–11 [29], Giaffreda *et al.* [30] have recently proposed a novel program that incorporates corrections to the degree of dissociation of such weak electrolytes as a function of the total prevailing ionic strength of the mixture according to the Debye–Hückel theory. We feel that the present version of our program has also evolved to such an extent to be a useful tool in laboratory work. It is a first approach at creating a "dry chemistry" (*e.g.*, computer modelling of the real CZE run) prior to the actual "wet chemistry" experiment.

6. Conclusions

Computer simulation in electrophoresis will become a more useful approach if in addition to the general pattern of the evolution it can predict the quantitative characteristics for a separation process. This work is an attempt to bring a new quantitative level to CZE modelling, when the experimental run is simulated with input data that are really used in everyday practice. The comparison of experimental and computer-simulated results was performed in terms of electropherograms displayed on the same scale as a temporary detector signal. This form of data presentation is the most natural way for experimenters, as it is usually implemented in commercial CZE units. Good coincidence of experimental and simulated concentration profiles and sample migration times gave one more validation for the mathematical model [8] underlying the computer code. We tried different substances, when their full and partial dissociation took place for samples consisting of one or more substances. The simulation data differed from those obtained in experiment by no more than a few per cent, which could be considered as satisfactory. At the same time the use of a simplified model with analytical solutions [11] gave much greater errors or even presented the wrong pattern of concentration profiles. Hence computer modelling confirmed again its power and usefulness.

Together with verification of the mathematical model for electrophoresis, the quantitative approach in computer simulation posed some questions that are of interest not only for modelling. Among them there are the problems of quantitative sample injection, the methods of recalculating the UV absorbance curves to concentration profiles and sample adsorption on the capillary walls. In this work we considered one of them. In order to quantify the UV absorbance electropherogram in terms of sample concentration two different methods were applied. They gave close but not coincident results. The reasons for the observed discrepancies should be the subject of separate studies, as also should the problem of interaction between the sample and the capillary wall. In this case the mathematical model needs modification to account for the sample adsorption.

7. Addendum

After this manuscript was accepted, we found an important review written by Hjertén [31] on the problem of quantitative analysis of peaks during electrophoresis in quartz tubes (I.D. 3 mm; O.D. 7.8 mm; present technology was not quite available in those days!). In pages 73–82 there is a thorough description on the problems of scanning a cylindrical object, on the relationship between absorbance and sample concen-

tration and on the accuracy of quantitative determinations, to which the reader is referred for additional information.

8. Acknowledgements

This work was supported in part by grants from the Agenzia Spaziale Italiana (ASI, Rome), the European Space Agency (ESA, Paris) and the Consiglio Nazionale delle Ricerche (CNR, Rome), Progetti Finalizzati Chimica Fine II and Biotecnologie e Biosensori. We thank Dr. M.S. Bello for helpful discussions and criticism.

9. References

[1] M. Bier, O.A. Palusinski, R.A. Mosher and D.A. Saville, *Science*, 219 (1983) 1281–1287.
[2] R.A. Mosher, W. Thormann and M. Bier, *J. Chromatogr.*, 320 (1985) 23–32.
[3] O.A. Palusinski, A. Graham, R.A. Mosher, M. Bier and D.A. Saville, *AIChE J.*, 32 (1986) 215–223.
[4] R.A. Mosher and W. Thormann, *Electrophoresis*, 11 (1990) 717–723.
[5] R.A. Mosher, D. Dewey, W. Thormann, D.A. Saville and M. Bier, *Anal. Chem.*, 61 (1989) 362–366.
[6] R.A. Mosher, P. Gebauer, J. Caslavska and W. Thormann, *Anal. Chem.*, 64 (1992) 2991–2997.
[7] R.A. Mosher, P. Gebauer and W. Thormann, *J. Chromatogr.*, 638 (1993) 155–164.
[8] R.A. Mosher, D.A. Saville and W. Thormann, *The Dynamics of Electrophoresis*, VCH, Weinheim, 1992.
[9] W. Thormann and R.A. Mosher, *Adv. Electrophoresis*, 2 (1988) 45–108.
[10] S.V. Ermakov, O.S. Mazhorova and Yu.P. Popov, *Informatica*, 3 (1992) 173–197.
[11] V. Šustáček, F. Foret and P. Boček, *J. Chromatogr.*, 545 (1991) 239–248.
[12] H. Poppe, *Anal. Chem.*, 64 (1992) 1908–1919.
[13] X. Huang, W.F. Coleman and R.N. Zare, *J. Chromatogr.*, 480 (1989) 95–110.
[14] S.E. Moring, in P.D. Grossman and J.C. Colburn (Editors), *Capillary Electrophoresis. Theory and Practice*, Academic Press, San Diego, 1992, Ch. 3, pp. 87–108.
[15] E.V. Dose and G. Guiochon, *Anal. Chem.*, 64 (1992) 123–128.
[16] S.V. Ermakov, O.S. Mazhorova and M.Yu. Zhukov, *Electrophoresis*, 13 (1992) 838–848.
[17] S.V. Ermakov, M.S. Bello and P.G. Righetti, *J. Chromatogr. A*, 661 (1994) 265–278.
[18] E. Grushka, R.M. McCormick and J.J. Kirkland, *Anal. Chem.*, 61 (1989) 241–246.
[19] A.E. Jones and E. Grushka, *J. Chromatogr.*, 466 (1989) 219–225.
[20] M.S. Bello and P.G. Righetti, *J. Chromatogr.*, 606 (1992) 103–111.
[21] M.S. Bello, E.I. Levin and P.G. Righetti, *J. Chromatogr.*, 652 (1993) 329–336.
[22] S. Hjertén, *Electrophoresis*, 11 (1990) 665–690.
[23] R.C. Weast (Editor), *CRC Handbook of Chemistry and Physics*, CRC Press, Boca Raton, FL, 67th ed., 1986–1987, pp. D159–D169.
[24] T. Hirokawa, M. Nishino and Y. Kiso, *J. Chromatogr.*, 252 (1982) 49–65.
[25] F.E.P. Mikkers, F.M. Everaerts and T.P.E.M. Verheggen, *J. Chromatogr.*, 169 (1979) 1–10.
[26] E. Grushka, in N. Catsimpoolas (Editor), *Methods of Protein Separation*, Vol. I, Plenum Press, New York, 1975, Ch. 6, pp. 161–192.
[27] W.J. Lambert and D.L. Middleton, *Anal. Chem.*, 62 (1990) 1585–1587.
[28] D.Y. Chen, H.P. Swerdlow, H.R. Harke, J.Z. Zhang and N.J. Dovichi, *J. Chromatogr.*, 559 (1991) 237–246.
[29] P.G. Righetti, *Immobilized pH Gradients: Theory and Methodology*, Elsevier, Amsterdam, 1990.
[30] E. Giaffreda, C. Tonani and P.G. Righetti, *J. Chromatogr.*, 630 (1993) 313–327.
[31] S. Hjertén, *Chromatogr. Rev.*, 9 (1967) 1–117.